JFE TECHNICAL REPORT
No. 6 (Oct. 2005)

Analysis of Motor Loss in Permanent Magnet Brushless Motors†

TODA Hiroaki[*1] WANG Jiabin[*2] HOWE David[*3]

Abstract:

This paper presents an analysis of the stator iron loss and the rotor eddy-current loss in 22-pole/24-slot modular and 24-pole/36-slot conventional permanent magnet brushless motors. The loss is evaluated by performing time-stepped finite element analysis. The no-load loss at 6 000 rpm is mainly due to the stator iron loss, while at rated load the eddy-current loss which is induced in the magnets is a major component of the total motor loss. It is shown that the no-load idling loss in the modular motor is lower than that of the conventional motor because it has fewer poles. On the other hand, the rotor eddy-current loss in the modular motor is higher because the stator armature magneto-motive force has low order spatial harmonic components. It is also shown that the idling loss in the stator can be reduced by ~50% by using 0.20 mm thick laminations rather than 0.35 mm laminations, whilst the eddy-current loss can be reduced significantly by segmenting the magnets circumferentially.

1. Introduction

There are growing concerns worldwide regarding global warming and environmental issues. There is a need, therefore, to reduce CO_2 emissions and to improve energy efficiency. Thus, the development and practical application of electric, fuel cell and hybrid electric vehicles is progressing rapidly in the automobile industry. Permanent magnet (PM) brushless motors have been widely used in such applications because of their smaller size and higher efficiency[1].

However, unlike induction motors, the time-varying magnetic field due to the permanent magnets results in a stator iron loss in PM motors even when they are operating on no-load. Thus, the no-load idling iron loss may significantly compromise the efficiency gain which is achieved by combining an electrical machine with an internal combustion engine. This is especially the case when the motor provides a torque boost only for short periods at low engine speeds to facilitate engine downsizing. Hence, it is necessary to minimize the stator iron loss by optimizing the motor design and employing a low loss lamination material (electrical steel sheets).

Permanent magnet brushless motors are being used in an ever-increasing range of applications due to their high efficiency and excellent dynamic performance. For motors having a conventional concentrated winding, the relationship between the rotor pole number p and the stator slot number N_s is given by:

$$N_s = 1.5 \times p$$

Recently, a relatively new topology of PM brushless motor, often referred to as "modular"[2,3], has emerged, which offers a number of significant advantages over conventional PM brushless motors. The pole-number/slot-number combinations for three-phase modular motors can be expressed by the following:

$$N_s = p \pm 1 \text{ or } p \pm 2, \text{ and } N_s \text{ must be divisible by 3.}$$

The stator winding of a modular PM motor differs from that of conventional brushless motors in that the coils which belong to one phase are concentrated and wound on consecutive teeth so that there is no over-

† Originally published in *JFE GIHO* No. 8 (June 2005), p. 17–21


*1 Senior Researcher,
Electrical Steel Res. Dept.,
Steel Res. Lab.,
JFE Steel


*2 Senior Lecturer,
Ph.D.,
Dept. of Electronic and Electrical Engineering,
Univ. of Sheffield,
U.K.


*3 Professor,
Ph.D.,
Dept. of Electronic and Electrical Engineering,
Univ. of Sheffield,
U.K.

lapping of phase windings. This is not only a distinct manufacturing advantage[4,5], but is also conducive to a high packing factor, and, hence, a high efficiency, and to reducing the likelihood of an inter-phase fault. It also results in a smaller number of slots per pole, e.g., 24 slots for a 22-pole modular motor as compared to 36 slots for a conventional 24-pole brushless motor, as illustrated in **Fig. 1**. Modular motors also yield a fractional number of slots per pole, with the smallest common multiple between the slot number and the pole number being relatively large. Consequently, the cogging torque can be extremely small without the use of skew [3,6].

Therefore, from the above standpoints, modular PM motors are considered to have advantages as potential candidates for torque boosting on hybrid vehicles. However, while the rotor eddy-current loss in conventional PM brushless ac motors is usually considered to be negligible, since high-order time harmonics in the stator current and space harmonics in the winding distribution are generally small, it is highly possible that a significant eddy-current loss can be generated in the permanent magnets of a modular motor. Since the stator magetomotive force (mmf) distribution contains a richer set of space harmonics, these harmonics can induce a significant eddy-current loss in the magnets, which may result in excessive heating[7,8]. Hence, it is important to compare the rotor eddy-current loss of modular and conventional topologies of PM brushless motor.

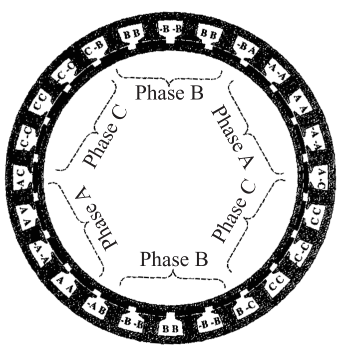

(a) Modular 22-pole/24-slot

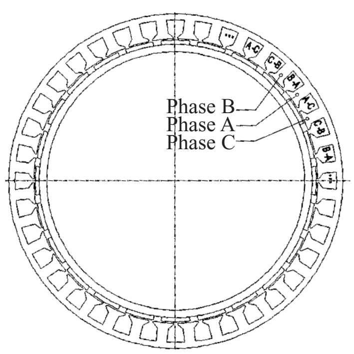

(b) Conventional 24-pole/36-slot

Fig. 1 Schematic of PM brushless motors

This paper presents an analysis and a method of reducing the no-load idling iron loss and the eddy-current loss in the rotor magnets of modular and conventional PM brushless motors.

2. Motor Design

Both modular 22-pole/24-slot and conventional 24-pole/36-slot surface-mounted PM motors, as illustrated in Fig. 1, have been designed to produce the same torque with the same peak current excitation at 1 700 rpm, viz. the maximum power point, within the same space envelope. **Table 1** shows the design specification and main parameters of both modular and conventional PM motors.

3. Analysis of No-load Iron Loss

3.1 Iron Loss Calculation

A time-stepped finite element analysis was conducted to obtain local flux density waveforms in each element of the stator lamination. The total iron loss in each element is the sum of the hysteresis component, the classical eddy-current component and the excess eddy-current component due to domain wall effects, and is given by[9,10]:

$$P_t = k_h f B_m^{\alpha} K(B_m) + (\sigma/12)(d^2 f/\delta)\int_{1/f}(\mathrm{d}B/\mathrm{d}t)^2\mathrm{d}t + k_e f\int_{1/f}\left|\mathrm{d}B/\mathrm{d}t\right|^{1.5}\mathrm{d}t$$

where

$$K(B_m) = 1 + (0.65/B_m)\Sigma\Delta B_i$$

ΔB_i is the variation in flux density during the excursion around a minor hysteresis loop. B_m and f are the peak flux density and the frequency, respectively, and σ, δ and d are the electrical conductivity, the mass density and the thickness of the laminations, respectively, k_h and α are hysteresis loss constants, and k_e is the excess eddy current loss constant. The loss constants k_h, α and k_e were determined by curve fitting iron loss data measured on Epstein size samples.

Table 1 Motor specifications and parameters

Topology	Modular	Conventional
Pole number	22	24
Slot number	24	36
Magnet resistivity ($\mu\Omega$·cm)	70	70
Peak current to produce 105 Nm torque (A)	500	500
Air-gap (mm)	1.6	1.6

Table 2 Magnetic properties of lamination materials

		35JN300	35JN210	20JNEH1200
Thickness, d	(mm)	0.35	0.35	0.20
Iron loss, $W_{15/50}$	(W/kg)	2.60	2.05	2.05
Iron loss, $W_{10/400}$	(W/kg)	18.0	16.0	11.0
Flux density, B_{50}	(T)	1.68	1.66	1.66

The iron loss due to rotational fluxes were calculated by summarising the losses due to the radial and circumferential flux density components[11]. **Table 2** shows the magnetic properties of the lamination materials which were considered.

3.2 No-load Iron Loss

The stator iron loss was calculated under a no-load condition at 6 000 rpm with the 35JN300 lamination material. **Figure 2** shows the iron loss density distribution in the modular and conventional motors. The total iron loss of the modular motor is lower than that of the conventional motor, although the iron loss density in the tooth tips of the modular design is larger than that of the conventional design.

Figure 3 compares the results of Fourier analysis of the flux density waveform in the tooth tips. The flux density waveform of the modular motor contain larger 3rd and 5th harmonics than those of the conventional motor, while the 7th, 9th, and 11th harmonic components are the almost same for both the modular and conventional motors. **Figure 4** shows the results of Fourier analysis of the flux density waveforms in the tooth body. The 3rd harmonic component in the modular motor is much larger than that of the conventional motor. However, the total iron loss of the modular motor is lower by about 15% than that of the conventional motor. This is because the modular motor has fewer poles than the conventional motor in order to achieve the same torque capability.

Figure 5 shows the influence of the lamination material on the stator iron loss. For the same motor topology, the iron losses are normalized to that of 0.35 mm material (35JN300). It is evident that the iron loss can be

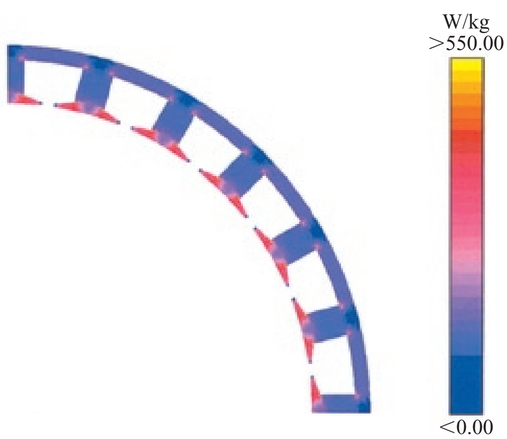

(a) Modular motor (Total iron loss = 1 176 W)

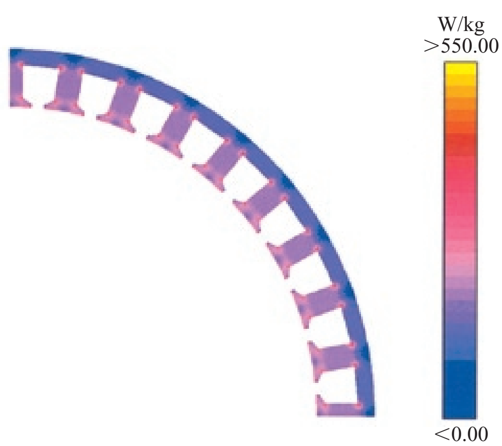

(b) Conventional motor (Total iron loss = 1 448 W)

Fig. 2 Iron loss distribution at 6 000 rpm on no-load

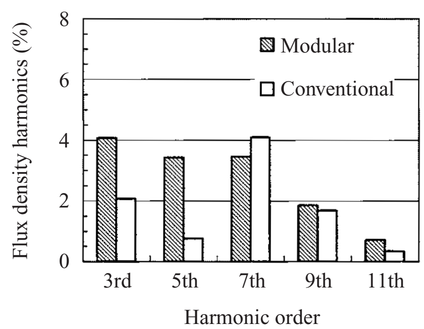

Fig. 3 Normalized flux density harmonics in a tooth tip

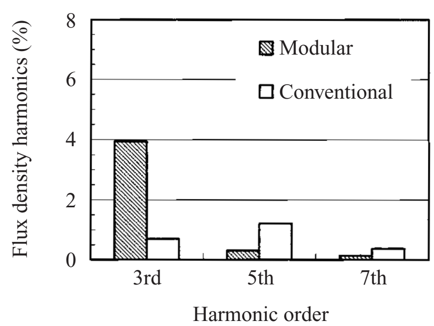

Fig. 4 Normalized flux density harmonics in a tooth body

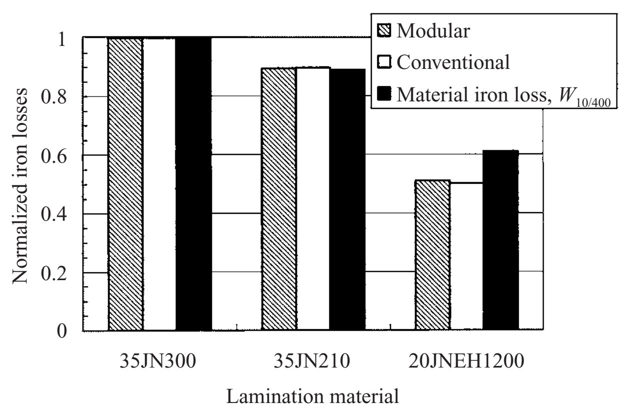

Fig. 5 Influence of lamination material on iron loss

reduced by ~50% by using 0.20 mm thick laminations rather than 0.35 mm laminations. Moreover, the variation of the calculated iron loss is in good agreement with that of the material iron loss $W_{10/400}$ (iron loss at 1.0 T, 400 Hz)[12]. Thus, the effect of lamination material on the iron loss can be easily evaluated by comparing their $W_{10/400}$ values.

4. Analysis of Eddy-current Loss in Rotor Magnets

4.1 Mageto-motive Force Harmonic Distribution of Stator Winding

The armature reaction mmf distribution can be derived analytically based on the assumption that the stator and rotor cores are infinitely permeable[13], and may be represented by a Fourier series, considering the winding arrangement shown in Fig. 1.

The stator winding is represented by an equivalent current sheet (J), which for a 3-phase motor is given by[7]:

$$J(\theta, t) = \begin{cases} \sum_{n}^{\infty} \frac{3}{2} J_n \cos(n\theta - p_r \omega t), & n = (3k + m) \\ \sum_{n}^{\infty} \left\{ -\frac{3}{2} J_n \cos(n\theta + p_r \omega t) \right\}, & n = (3k - m) \\ 0, & n \neq 3k \pm m \end{cases}$$

where n is the harmonic order, p_r is the rotor pole-pair number, ω is the rotor angular velocity, and

$$J_n = \frac{2N_s I_m}{\pi R_s} K_{wn},$$

where N_s, I_m, and R_s are the number of series turns per phase, the peak phase current and the stator bore inner radius, respectively, and K_{wn} is the winding factor. The value (± 1) for m is dependent on the winding configuration. For the 22-pole/24-slot modular motor $m = -1$, while for the 24-pole/36-slot conventional motor $m = 1$.

Figure 6 (a) shows the space harmonic mmf distribution for the modular 22-pole/24-slot motor winding normalised to the ampere-turns per slot, while Fig. 6 (b) shows the mmf distribution for the conventional 24-pole/36-slot motor. As can be seen, the stator winding mmf distribution in the modular motor contains a rich set of harmonics. It is evident that the 11th, 13th, 35th, 37th, ..., harmonics are dominant, while there exist low order harmonics such as the 5th, 7th, 17th, and 19th, etc. For the modular motor, however, only the 11th mmf harmonic interacts with the magnetic field of the 22-pole permanent magnet rotor to produce continuous torque. The other harmonics, especially low order harmonics

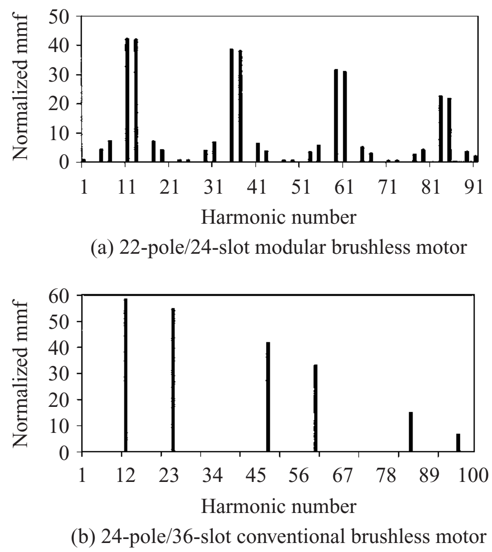

Fig. 6 Normalized magneto-motive force (mmf) space harmonic distributions

such as the 5th, 7th, and 13th, can cause a significant eddy-current loss in the magnets[14].

4.2 Rotor Eddy-current Loss

The eddy-current loss in the magnets was calculated under various conditions at 1 700 rpm by time-stepped FE analysis. Furthermore, the presence of stator slot openings causes a variation of the magnetic field in the magnets[15], this component of rotor eddy-current loss being dependent on the width of the slot openings and the pole/slot number combination. Hence, FE analysis was undertaken to examine the effect of the slot openings on the eddy-current loss.

Figures 7 and **8** show the influence of the number of circumferential magnet segments per pole on the eddy-current loss of the modular and conventional motors, respectively, when both are supplied with sinusoidal phase current waveforms. It will be seen that a significant eddy-current loss is produced in both the modular and conventional motors when the number of magnet segments is one per pole. As can be seen, circumferential segmentation of the magnets is effective in reducing the eddy-current loss, 2 or 4 segments per pole being necessary to keep the eddy-current loss to a reasonably low level even in the conventional motor.

FE calculations with the magnets unmagnetized show the eddy-current loss caused by the stator mmf space harmonics, while FE results under a no-load (or open-circuit) condition represent the eddy-current loss due to the slot openings only. It can be seen that the eddy-current loss associated with the stator mmf for the modular motor is larger than that for the conventional motor. However, it will also be noted that while the eddy-current loss due to the slot openings is relatively small for the modular motor, it is significant for the conventional motor. It will also be observed that the total

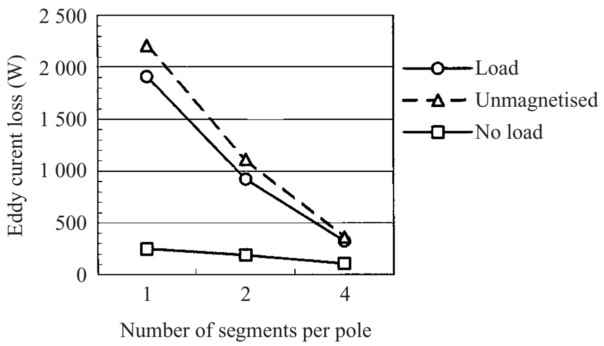

Fig. 7 Influence of number of magnet segments per pole on eddy-current loss for modular motor

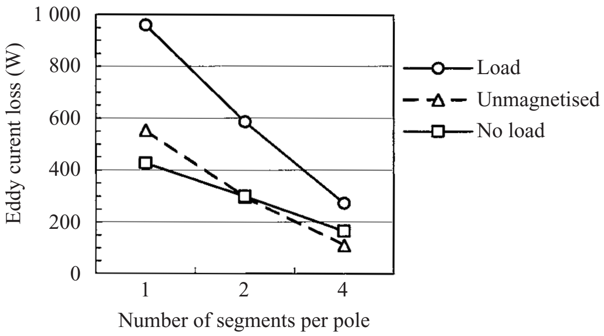

Fig. 8 Influence of number of magnet segments per pole on eddy-current loss for conventional motor

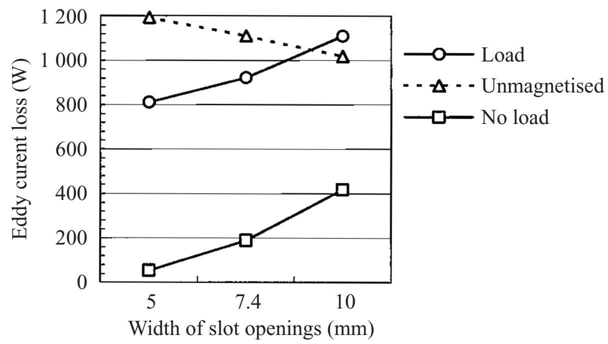

Fig. 9 Influence of slot opening on eddy-current loss for modular motor (Number of magnet segments per pole: 2)

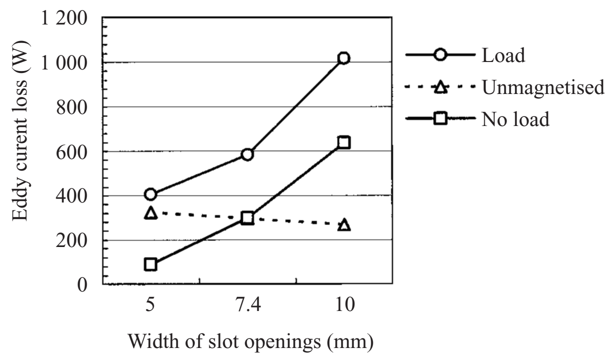

Fig. 10 Influence of slot opening on eddy-current loss for conventional motor (Number of magnet segments per pole: 2)

eddy-current loss at rated load does not equal the sum of the losses calculated separately on no-load and with the magnets unmagnetized, due to the influence of skin effect and saturation.

Figures 9 and **10** show the variation of the eddy-current loss in the magnets with the width of the stator slot openings for the modular and conventional motors, respectively. It can be seen that the eddy-current loss on both full-load and no-load conditions increases with an increase in the width of the slot openings for both the modular and conventional motors. Since the frequency of the flux variation is proportional to the number of slots, the effect of the slotting on the eddy-current loss in the conventional motor is more significant than that in the modular motor. Therefore, in addition to their influence on the cogging torque and synchronous inductance, the effect of the slot openings on the eddy-current loss in the permanent magnets may have to be considered during the design stage, especially for a conventional topology of motor.

Furthermore, since 2 or 4 magnet segments per pole are necessary to avoid excessive heating of the magnets for both modular and conventional motors, it may be concluded that the modular motor design is much better from the standpoint of motor performance.

5. Conclusions

The no-load idling iron loss and the rotor eddy-current loss in modular and conventional topologies of PM motors, which have been designed to produce the same torque with the same peak current, have been analyzed by FE calculations. The no-load iron loss of the modular motor is lower than that of the conventional motor because the modular motor has fewer poles in order to achieve the same power capability. The idling loss can be reduced by about half by using 0.20 mm thick laminations rather than 0.35 mm laminations. The rotor eddy-current loss in the modular motor is higher because the stator armature magneto-motive force has low order spatial harmonic components. However, the eddy-current loss in the magnets can be reduced significantly by segmenting the magnets circumferentially. Even in the conventional motor, 2 or 4 magnet segments per pole are necessary to avoid excessive heating, and the eddy-current loss due to the stator slot openings in the conventional motor is more significant than that in the modular motor. Therefore, it is concluded that the modular motor is much better in that it has a lower total motor loss.

This research was carried out in the Department of Electronic & Electrical Engineering, University of Sheffield, U.K. when H. Toda was on leave from JFE Steel. The authors wish to thank Dr. Atallah and Dr. Xia in the

University of Sheffield for helpful suggestions.

References

1) Sasaki, M. Hybrid vehicle technology-current status and future challenges. Preprints of JSAE Cong. no. 20045325.
2) Atallah, K.; Howe, D. Modular permanent magnet brushless machines for aerospace and automotive applications. Proc. 20th International Workshop on Rare-earth Magnets and their Applications. 2000, p. 1039–1048.
3) Atallah, K.; Wang, J.; Howe, D. Torque ripple minimisation in modular permanent magnet brushless machines. IEEE Trans. on Industry Applications. vol. 39, 2003, p. 1689–1695.
4) Oikawa, T.; Tajima, T.; Matsumoto, K.; Akita, H.; Kawaguchi, H.; Kometani, H. Development of high efficiency brushless DC motor with new manufacturing method of stator for compressors. in Proc. 16th Inter. Compressor Eng. Conf. CD12-4, 2002.
5) Jack, A.G.; Mecrow, B.C.; Dickinson, P.G.; Stephenson, D. Permanent-magnet machines with powdered iron cores and prepressed windings, IEEE Trans. Ind. Applications. vol. 36, 2003, p. 1077–1084.
6) Ohnishi, K. Cogging torque reduction in permanent magnet brushless motors. T. IEE Jpn. vol. 122-D, no. 4, 2002, p. 338–345.
7) Atallah, K.; Howe, D.; Mellor, P. H.; Stone, D. A. Rotor loss in permanent magnet brushless AC machines. IEEE Trans. on Industry Applications. vol. 36, 2000, p. 1612–1618.
8) Nakano, M.; Kometani, H. A study on eddy-current losses in rotors of surface permanent magnet synchronous motors. Papers of Technical Meeting on Rotating Machinery. IEE Jpn. RM-03-73, 2003, p. 7–12.
9) Bertotti, G. General properties of power losses in soft ferromagnetic materials. IEEE Trans. on Magnetics. vol. 24, 1988, p. 621–630.
10) Fiorillo, F.; Novikov, A. An improved approach to power losses in magnetic laminations under non-sinusoidal induction waveform. IEEE Trans. on Magnetics. vol. 26, 1990, p. 2904–2910.
11) Atallah, K.; Zhu, Z. Q.; Howe, D. An improved method for predicting iron losses in brushless permanent magnet dc drives. IEEE Trans. on Magnetics. vol. 28, 1992, p. 2997–2999.
12) Honda, A.; Senda, K.; Sadahiro, K. Electrical steel for motors of electric and hybrid vehicles. Kawasaki Steel Giho. vol. 34, no. 2, 2002, p. 85–89.
13) Zhu, Z. Q.; Howe, D. Instantaneous magnetic field distribution in brushless permanent dc motors —Part II: Armature reaction field. IEEE Trans. on Magnetics. vol. 29, 1993, p. 136–142.
14) Toda, H.; Xia, Z. P.; Wang, J.; Atallah, K.; Howe, D. Rotor eddy-current loss in permanent magnet brushless machines. IEEE Trans. on Magnetics. vol. 40, 2004, p. 2104–2106.
15) Matsuoka, K.; Kondoh, K.; Kobayashi, Y.; Shiraishi, S. Development of wheel mounted direct drive traction motor for rail vehicle. T. IEE Jpn. vol. 121-D, no. 11, 2001, p. 1176–1184.